Joint assessment of brain and spinal cord motor tract damage in patients with early RRMS : predominant impact of spinal cord lesions on motor function

Raphaël Chouteau

THÈSE D'EXERCICE / UNIVERSITÉ DE RENNES 1
sous le sceau de l'Université Bretagne Loire

Thèse en vue du

DIPLÔME D'ÉTAT DE DOCTEUR EN MÉDECINE

présentée par

Raphaël CHOUTEAU

Né le 10/05/1989 à Rennes

Évaluation conjointe des lésions du tractus moteur du cerveau et de la moelle épinière chez les patients atteints de SEP débutante: impact prédominant des lésions de la moelle épinière sur la fonction motrice

Thèse soutenue à Rennes

Le 12/07/2019

devant le jury composé de :

Gilles EDAN
PU-PH CHU de Rennes/ *président de jury*
Benoit COMBES
PhD, Post doctorant + INRIA Rennes/ *examinateur*
Paul SAULEAU
PU-PH CHU de Rennes / *examinateur*
Jean-Christophe FERRE
PU-PH CHU de Rennes / *examinateur*
Anne KERBRAT
PH-U CHU de Rennes/ *directrice de thèse*

PROFESSEURS DES UNIVERSITES

NOM	PRENOM	TITRE	CNU
ANNE-GALIBERT	Marie-Dominique	PU-PH	Biochimie et biologie moléculaire
BARDOU-JACQUET	Edouard	PU-PH	Gastroentérologie ; hépatologie ; addictologie
BELAUD-ROTUREAU	Marc-Antoine	PU-PH	Histologie ; embryologie et cytogénétique
BELLISSANT	Eric	PU-PH	Pharmacologie fondamentale ; pharmacologie clinique ; addictologie
BELOEIL	Hélène	PU-PH	Anesthésiologie-réanimation et médecine péri-opératoire
BENDAVID	Claude	PU-PH	Biochimie et biologie moléculaire
BENSALAH	Karim	PU-PH	Urologie
BEUCHEE	Alain	PU-PH	Pédiatrie
BONAN	Isabelle	PU-PH	Médecine physique et de réadaptation
BONNET	Fabrice	PU-PH	Endocrinologie, diabète et maladies métaboliques ; gynécologie médicale
BOUDJEMA	Karim	PU-PH	Chirurgie générale
BOUGET	Jacques	Pr Emérite	Thérapeutique-médecine de la douleur ; addictologie
BOUGUEN	Guillaume	PU-PH	Gastroentérologie ; hépatologie ; addictologie
BRASSIER	Gilles	PU-PH	Neurochirurgie
BRISSOT	Pierre	Pr Emérite	Gastroentérologie ; hépatologie ; addictologie
CARRE	François	PU-PH	Physiologie
CATROS	Véronique	PU-PH	Biologie cellulaire
CATTOIR	Vincent	PU-PH	Bactériologie-virologie ; hygiène hospitalière
CHALES	Gérard	Pr Emérite	Rhumatologie
CORBINEAU	Hervé	PU-PH	Chirurgie thoracique et cardiovasculaire
CUGGIA	Marc	PU-PH	Biostatistiques, informatique médicale et technologies de communication
DARNAULT	Pierre	PU-PH	Anatomie
DAUBERT	Jean-Claude	Pr Emérite	Cardiologie
DAVID	Véronique	PU-PH	Biochimie et biologie moléculaire
DAYAN	Jacques	Pr Associé	Pédopsychiatrie ; Addictologie
DE CREVOISIER	Renaud	PU-PH	Cancérologie ; radiothérapie
DECAUX	Olivier	PU-PH	Médecine interne ; gériatrie et biologie du vieillissement ; addictologie
DESRUES	Benoît	PU-PH	Pneumologie ; addictologie

DEUGNIER	Yves	Pr Emérite	Gastroentérologie ; hépatologie ; addictologie
DONAL	Erwan	PU-PH	Cardiologie
DRAPIER	Dominique	PU-PH	Psychiatrie d'adultes ; addictologie
DUPUY	Alain	PU-PH	Dermato-vénérologie
ECOFFEY	Claude	PU-PH	Anesthésiologie-réanimation et médecine péri-opératoire
EDAN	Gilles	PU-PH consultant	Neurologie
FERRE	Jean-Christophe	PU-PH	Radiologie et imagerie médicale
FEST	Thierry	PU-PH	Hématologie ; transfusion
FLECHER	Erwan	PU-PH	Chirurgie thoracique et cardiovasculaire
GANDEMER	Virginie	PU-PH	Pédiatrie
GANDON	Yves	PU-PH	Radiologie et imagerie médicale
GANGNEUX	Jean-Pierre	PU-PH	Parasitologie et mycologie
GARIN	Etienne	PU-PH	Biophysique et médecine nucléaire
GAUVRIT	Jean-Yves	PU-PH	Radiologie et imagerie médicale
GODEY	Benoît	PU-PH	Oto-rhino-laryngologie
GUGGENBUHL	Pascal	PU-PH	Rhumatologie
GUILLE	François	PU-PH	Urologie
GUYADER	Dominique	PU-PH	Gastroentérologie ; hépatologie ; addictologie
HAEGELEN	Claire	PU-PH	Anatomie
HOUOT	Roch	PU-PH	Hématologie ; transfusion
JEGO	Patrick	PU-PH	Médecine interne ; gériatrie et biologie du vieillissement ; addictologie
JEGOUX	Franck	PU-PH	Oto-rhino-laryngologie
JOUNEAU	Stéphane	PU-PH	Pneumologie ; addictologie
KAYAL	Samer	PU-PH	Bactériologie-virologie ; hygiène hospitalière
LAMY DE LA CHAPELLE	Thierry	PU-PH	Hématologie ; transfusion
LAVIOLLE	Bruno	PU-PH	Pharmacologie fondamentale ; pharmacologie clinique ; addictologie
LAVOUE	Vincent	PU-PH	Gynécologie-obstétrique ; gynécologie médicale
LE BRETON	Hervé	PU-PH	Cardiologie
LE GUEUT	Mariannick	PU-PH consultant	Médecine légale et droit de la santé
LE TULZO	Yves	PU-PH	Médecine intensive-réanimation
LECLERCQ	Christophe	PU-PH	Cardiologie
LEDERLIN	Mathieu	PU-PH	Radiologie et imagerie médicale
LEGUERRIER	Alain	Pr Emérite	Chirurgie thoracique et cardiovasculaire
LEJEUNE	Florence	PU-PH	Biophysique et médecine nucléaire
LEVEQUE	Jean	PU-PH	Gynécologie-obstétrique ; gynécologie médicale

LIEVRE	Astrid	PU-PH	Gastroentérologie ; hépatologie ; addictologie
MABO	Philippe	PU-PH	Cardiologie
MAHE	Guillaume	PU-PH	Chirurgie vasculaire ; médecine vasculaire
MALLEDANT	Yannick	Pr Emérite	Anesthésiologie-réanimation et médecine péri-opératoire
MENER	Eric	Pr Associé	Médecine générale
MEUNIER	Bernard	PU-PH	Chirurgie digestive
MICHELET	Christian	Pr Emérite	Maladies infectieuses ; maladies tropicales
MOIRAND	Romain	PU-PH	Gastroentérologie ; hépatologie ; addictologie
MORANDI	Xavier	PU-PH	Anatomie
MOREL	Vincent	Pr Associé	Médecine palliative
MOSSER	Jean	PU-PH	Biochimie et biologie moléculaire
MOURIAUX	Frédéric	PU-PH	Ophtalmologie
MYHIE	Didier	Pr Associé	Médecine générale
ODENT	Sylvie	PU-PH	Génétique
OGER	Emmanuel	PU-PH	Pharmacologie fondamentale ; pharmacologie clinique ; addictologie
PARIS	Christophe	PU-PH	Médecine et santé au travail
PERDRIGER	Aleth	PU-PH	Rhumatologie
PLADYS	Patrick	PU-PH	Pédiatrie
RAVEL	Célia	PU-PH	Histologie, embryologie et cytogénétique
REVEST	Matthieu	PU-PH	Maladies infectieuses ; maladies tropicales
RICHARD DE LATOUR	Bertrand	Pr Associé	Chirurgie thoracique et cardiovasculaire
RIFFAUD	Laurent	PU-PH	Neurochirurgie
RIOUX-LECLERCQ	Nathalie	PU-PH	Anatomie et cytologie pathologiques
ROBERT-GANGNEUX	Florence	PU-PH	Parasitologie et mycologie
ROPARS	Mickaël	PU-PH	Chirurgie orthopédique et traumatologique
SAINT-JAMES	Hervé	PU-PH	Biophysique et médecine nucléaire
SAULEAU	Paul	PU-PH	Physiologie
SEGUIN	Philippe	PU-PH	Anesthésiologie-réanimation et médecine péri-opératoire
SEMANA	Gilbert	PU-PH	Immunologie
SIPROUDHIS	Laurent	PU-PH	Gastroentérologie ; hépatologie ; addictologie
SOMME	Dominique	PU-PH	Médecine interne ; gériatrie et biologie du vieillissement ; addictologie
SOULAT	Louis	Pr Associé	Médecine d'urgence
SULPICE	Laurent	PU-PH	Chirurgie générale
TADIE	Jean Marc	PU-PH	Médecine intensive-réanimation
TARTE	Karin	PU-PH	Immunologie
TATTEVIN	Pierre	PU-PH	Maladies infectieuses ;

			maladies tropicales
TATTEVIN-FABLET	Françoise	Pr Associé	Médecine générale
THIBAULT	Ronan	PU-PH	Nutrition
THIBAULT	Vincent	PU-PH	Bactériologie-virologie ; hygiène hospitalière
THOMAZEAU	Hervé	PU-PH	Chirurgie orthopédique et traumatologique
TORDJMAN	Sylvie	PU-PH	Pédopsychiatrie ; addictologie
VERHOYE	Jean-Philippe	PU-PH	Chirurgie thoracique et cardiovasculaire
VERIN	Marc	PU-PH	Neurologie
VIEL	Jean-François	PU-PH	Epidémiologie, économie de la santé et prévention
VIGNEAU	Cécile	PU-PH	Néphrologie
VIOLAS	Philippe	PU-PH	Chirurgie infantile
WATIER	Eric	PU-PH	Chirurgie plastique, reconstructrice et esthétique ; brûlologie
WODEY	Eric	PU-PH	Anesthésiologie-réanimation et médecine péri-opératoire

MAITRES DE CONFERENCES DES UNIVERSITES

NOM	PRENOM	TITRE	CNU
ALLORY	Emmanuel	MC Associé	Médecine générale
AME-THOMAS	Patricia	MCU-PH	Immunologie
AMIOT	Laurence	MCU-PH	Hématologie ; transfusion
ANSELMI	Amédéo	MCU-PH	Chirurgie thoracique et cardiovasculaire
BEGUE	Jean Marc	MCU-PH	Physiologie
BERTHEUIL	Nicolas	MCU-PH	Chirurgie plastique, reconstructrice et esthétique ; brûlologie
BOUSSEMART	Lise	MCU-PH	Dermato-vénéréologie
BROCHARD	Charlène	MCU-PH	Physiologie
CABILLIC	Florian	MCU-PH	Biologie cellulaire
CAUBET	Alain	MCU-PH	Médecine et santé au travail
CHHOR-QUENIART	Sidonie	MC Associé	Médecine générale
DAMERON	Olivier	MCF	Informatique
DE TAYRAC	Marie	MCU-PH	Biochimie et biologie moléculaire
DEGEILH	Brigitte	MCU-PH	Parasitologie et mycologie
DROITCOURT	Catherine	MCU-PH	Dermato-vénéréologie
DUBOURG	Christèle	MCU-PH	Biochimie et biologie moléculaire
DUGAY	Frédéric	MCU-PH	Histologie, embryologie et cytogénétique
EDELINE	Julien	MCU-PH	Cancérologie ; radiothérapie
FIQUET	Laure	MC Associé	Médecine générale
GARLANTEZEC	Ronan	MCU-PH	Epidémiologie, économie de la santé et prévention
GOUIN épouse THIBAULT	Isabelle	MCU-PH	Hématologie ; transfusion
GUILLET	Benoit	MCU-PH	Hématologie ; transfusion
JAILLARD	Sylvie	MCU-PH	Histologie, embryologie et cytogénétique
KALADJI	Adrien	MCU-PH	Chirurgie vasculaire ; médecine vasculaire
KAMMERER-JACQUET	Solène-Florence	MCU-PH	Anatomie et cytologie pathologiques
LAVENU	Audrey	MCF	Sciences physico-chimiques et ingénierie appliquée à la santé
LE GALL	François	MCU-PH	Anatomie et cytologie pathologiques
LE GALL	Vanessa	MC Associé	Médecine générale
LEMAITRE	Florian	MCU-PH	Pharmacologie fondamentale ; pharmacologie clinique ; addictologie
MARTINS	Pédro Raphaël	MCU-PH	Cardiologie
MATHIEU-SANQUER	Romain	MCU-PH	Urologie
MENARD	Cédric	MCU-PH	Immunologie
MICHEL	Laure	MCU-PH	Neurologie
MOREAU	Caroline	MCU-PH	Biochimie et biologie moléculaire
MOUSSOUNI	Fouzia	MCF	Informatique
NAUDET	Florian	MCU-PH	Thérapeutique-médecine de la douleur ; addictologie
PANGAULT	Céline	MCU-PH	Hématologie ; transfusion

RENAUT	Pierrick	MC Associé	Médecine générale
ROBERT	Gabriel	MCU-PH	Psychiatrie d'adultes ; addictologie
SCHNELL	Frédéric	MCU-PH	Physiologie
THEAUDIN épouse SALIOU	Marie	MCU-PH	Neurologie
TURLIN	Bruno	MCU-PH	Anatomie et cytologie pathologiques
VERDIER épouse LORNE	Marie-Clémence	MCU-PH	Pharmacologie fondamentale ; pharmacologie clinique ; addictologie
ZIELINSKI	Agata	MCF	Philosophie

Remerciements

Au Professeur EDAN, pour sa disponibilité et surtout son perpétuel enthousiasme,

Au Professeur SAULEAU, pour son apprentissage à la rigueur scientifique et professionnelle,

Au Professeur FERRE, pour m'avoir accordé sa confiance pour ce projet,

Au Dr COMBES (PhD), pour sa curiosité et pour m'avoir patiemment initier à l'informatique,

Au Dr KERBRAT, pour son soutien constant et éclairé, en dépit des distances

Dédicaces

Au Professeur Marc VERIN pour m'avoir orienté vers la neurologie à la sortie des ECN,

Aux Docteurs KASSIOTIS et PINEL qui m'ont transmis leur passion du diagnostic,

A Thierry, Karine, Timothée, Rabab et Emmanuel pour m'avoir tant appris sur « le nerf » et « le muscle »,

À toute l'équipe « Visages », en particulier Élise, pour m'avoir aidé pendant de longues heures de galère devant « mon » Linux,

A mes parents, pour leur soutien sans faille tout au long de mes études et qui doivent se réjouir au terme de mes études…

A mon frère et à mes sœurs, à ma belle-sœur, à mon beau-frère, à mes neveux, à ma nièce, et à tous mes amis, qui me rappellent que le travail n'est pas toute la vie

A mes co-internes pour tous ces moments passés au travail mais surtout en dehors, certains sont d'ailleurs devenus de véritables amis

Et surtout merci à ma compagne Pauline, pour son amour, sa patience et ses encouragements

Table des matières

II) Documents administratifs	Pages 2-11
> Liste des PU-PH et MCU-PH.	Page 3
> Remerciements et dédicaces	Page 8
> Table des matières.	Page 9
> Liste des documents annexes	Page 10
> Liste des illustrations	Page 11
III) Corps de thèse.	Pages 12-40
> Page de titre	Page 12
> Introduction.	Page 13
> Méthode.	Page 14
> Résultats.	Page 18
> Discussion	Page 20
> Conclusion.	Page 22
> Bibliographie.	Page 23
> Figures	Page 26
> Tableaux	Page 29
IV) Documents annexes.	Pages 41-47
V) Résumé.	Page 48

Liste des documents annexes

Annexe 1: Appendix for MRI methodology	**Pages 41-45**
Annexe 2: Appendix for electrophysiology methodology	**Pages 46-47**

Liste des illustrations

Figure 1: Study design.	**Page 26**
Figure 2: Example of spinal cord MRI in a patient with RMMS.	**Page 27**
Figure 3: Example of brain MRI in patient with RRMS.	**Page 28**

Joint assessment of brain and spinal cord motor tract damage in patients with early RRMS: predominant impact of spinal cord lesions on motor function

Raphaël Chouteau[1,2], Benoit Combès[2] (PhD), Elise Bannier[2,3] (PhD), Haykel Snoussi[2], Jean Christophe Ferré[2,3] (MD, PhD), Christian Barillot[2] (PhD), Gilles Edan[1,2,4] (MD, PhD), Paul Sauleau[5,6] (MD, PhD), Anne Kerbrat (MD, PhD)[1,2]

[1]CHU Rennes, Neurology Department, Rennes, France;

[2]Univ Rennes, Inria, CNRS, Inserm, IRISA UMR 6074, Visages U1228, France;

[3]CHU Rennes, Radiology Department, Rennes, France;

[4]Plurithematic Clinical Investigation Center (CIC-P 1414), INSERM, Rennes, France;

[5]CHU Rennes, Neurophysiology Department, France;

[6]Behavior and Basal Ganglia research unit (EA4712), Rennes 1 University, Rennes, France.

Introduction

The secondary progressive phenotype MS usually presents as a worsening pyramidal syndrome of both lower and upper limbs, suggesting strong corticospinal tracts (CST) involvement[1]. However, quantifying focal and diffuse CST damage from the motor cortex to the spinal cord (SC) using MRI presents data-acquisition and data-processing challenges. Thus, the whole CST has not yet been explored in patients with MS.

Conversely, a substantial number of studies have focused on the brain portion of the CST. Diffusion tensor imaging (DTI) is a tool of choice for this exploration, as it allows white-matter (WM) tracts to be extracted and tissue integrity to be characterized. In particular, DTI-derived metrics extracted from the brain CST have been shown to correlate to several clinical scores[2,3,4]. Moderate associations between motor function and T2 lesion volume in the CST have been reported[5]. Finally, CST T2 lesion volume has been shown to correlate with DTI metrics in normal-appearing CST[6], suggesting that focal damage plays a role in both the lesion and Wallerian degeneration.

By contrast, only a limited number of studies have evaluated the impact of CST damage in the SC. For a start, the precise location of the lesions had not been fully explored, owing to technical limitations[7], including the small size of the WM tract in the SC and the need for systematic whole-cord axial acquisitions with high in-plane resolution and large coverage[7]. Nevertheless, even without a specific assessment of lesion location, the SC T2 lesion load has been shown to be associated with disability[8], and to have a strong prognostic value[9,10]. A few studies have also highlighted the involvement of diffuse SC CST damage in motor disabilities. In particular, magnetization transfer imaging metrics in the lateral column of the SC have been found to be correlated with ankle flexion strength[11], and diffusion imaging metrics with scores on the Expanded Disability Status Scale (EDSS), 9-Hole Peg Test (9HPT) and Timed 25-Foot Walk (T25FW)[12].

In the present study, we took advantage of advances in SC MRI acquisition and post-processing to assess CST structural integrity in both the cortex and the cervical SC, and examine their relative associations with motor function in a population of patients with early relapsing-remitting MS (RRMS). Structural integrity was assessed using T2 lesion delineations and DTI quantitative measurements in the brain and cervical SC. In addition to standard clinical scores, which are usually slightly impacted at this stage of the disease[13], we also assessed upper-limb motor functions by electrophysiology in a subset of patients. More specifically, we recorded the central motor conduction time (CMCT) using transcranial magnetic stimulation, whose increase suggests demyelination[14] or loss of rapidly

conducting corticospinal fibres, as well as the triple stimulation technique (TST) amplitude ratio, whose decrease suggests central conduction block or axonal loss[15,16].

Methods

Participants

We included 44 patients with early RRMS in this single-center study. All patients underwent an MRI evaluation, and 24 also underwent an electrophysiological evaluation (on a voluntary basis). They were part of a multicenter longitudinal study (EMISEP; ClinicalTrials ID: NCT02117375) approved by the relevant institutional review board. Written informed consent was obtained from all participants. The main inclusion criteria were 1) age 18-45 years, 2) RRMS diagnosis according to 2010 criteria[17] < 48 months, 3) initial MRI severity > 9 T2 lesions on brain MRI and/or initial myelitis documented on spinal cord MRI, and 4) no relapse and no corticosteroids in the month before inclusion. Healthy controls were also included for brain (n = 16) and spinal cord MRI (n = 19) assessment. The demographic characteristics of patients and controls are summarized in Supplementary Table 1.

Study design

The study design is described below and summarized in Figure 1.

MRI acquisitions

Imaging was performed using a 3-tesla MRI scanner (MAGNETOM Verio (VB17), Siemens). Details of acquisition parameters are given in Supplemental Material. Briefly: 1) for SC lesion identification, axial T2*w and sagittal T2 TSE from C1 to C7; 2) for SC diffusion measurement, diffusion-weighted EPI sequence (30 directions); 3) for brain lesion identification, axial T2w, axial PD, and 3D FLAIR; and 4) for brain CST identification and diffusion measurements, diffusion-weighted EPI sequence (30 directions) and 3DT1 MPRAGE.

MRI processing

Processing was performed using the Spinal Cord Toolbox (SCT Version 3.0)[18] and the Anima toolbox[19]. Details of image analysis are given in Supplemental Material and are summarized below for the patients' scans. The same steps were applied to the controls' scans, except for those concerning lesion identification and alignment.

Spinal cord MRI processing:

- **Lesion volume fractions:** First, two neurologists (RC, AK) manually delineated cervical cord lesions on the axial T2*w images, using sagittal T2w images to help identify the lesions. Second, the SC was segmented and the vertebrae labelled on the T2*w images. Third, the left and right lateral and ventral components of the CST were extracted using the MNI-Poly-AMU template (Fig. 2). Fourth, the lesion volume fraction was computed as (lesion volume in region of interest) / (ROI volume), with ROIs in the cervical cord defined as right CST, left CST, whole CST, and whole cord. CST sides were named according to their functional lateralization (e.g., the right CST related to motor function on the right side of the body). Level C7 (bottom of the acquisition slab) was removed from this analysis, owing to the difficulty of precisely aligning them on the template.

- **Scalar diffusion parameters:** First, we corrected the diffusion images for motion and distortion. Second, we applied cord segmentation, level labelling and ROI extraction to the mean diffusion B0 images to locate the left and right lateral CST components in the diffusion acquisition frame. Because of the low resolution of our DTI data, ventral CST components were not extracted, to avoid a detrimental partial volume effect. Third, we extracted the fractional anisotropy (FA), radial diffusivity (RD) and axial diffusivity (AD) maps. Finally, for each participant, the mean values of diffusion parameters for the CST, spine and lesions were extracted for the C2-C4 ROI. We selected this ROI because we judged it to be the least prone to strong geometric distortion and variability in terms of DTI parameters in our control group.

Brain MRI processing:

- **Lesion volume fractions:** First, two neurologists (RC, AK) manually performed lesion delineation on the 3D-FLAIR images, using T2w and PD images to help lesion identification. Second, diffusion acquisitions were corrected for motion and distortion. Third, lesion masks were rigidly aligned to the diffusion

acquisitions. Fourth, the WM mask was extracted. Fifth, brain portions of the left and right CSTs were identified after masking out WM lesions, using probabilistic tractography and a set of filtering ROIs (Fig. 3). Finally, for each patient, we computed the lesion volume fractions in the right CST, left CST, whole CST, and whole brain. Lesion fractions were also computed on similar ROIs combining lesion volumes from both the brain and SC.

- **Scalar diffusion parameters:** The FA, RD and AD parameters were then extracted from the diffusion acquisitions. Finally, for each participant, each of these DTI parameters was averaged on the brain CST, WM, normal-appearing WM, and lesions.

Electrophysiological acquisitions

The electrophysiological acquisition protocol is fully described in Supplemental Material. Briefly, motor evoked potentials (MEPs), TST amplitude ratio and area measurements were performed on the first dorsal interosseous muscle on each side, using surface electrodes and standard protocols[20,21]. Values > 8 ms for the CMCT, < 33% for the MEP ratio, < 93% for the TST ratio, and < 92% for the TST area were considered as abnormal[15,20].

Clinical data

The clinical assessment included the 1) EDSS and pyramidal EDSS, 2) 9HPT, 3) T25FW, 4) 6-minute walking test (6MWT), and 5) MS walking scale (MSW12).

Statistical analysis

Statistical analysis was performed in R (Version 3.4.4)[22]. We used a 0.05 testwise significance level (no correction for multiple comparisons).

Differences in mean DTI metrics between patients and controls for the different ROIs and diffusion parameters and differences in mean electrophysiological scores between sides with and without pyramidal signs were tested by computing the p value associated with the equality of means using Welch's two-sample t test.

Correlations between lesion volume fractions in the brain and cord were assessed using the Pearson correlation coefficient. The associated p values for $r = 0$ are also given.

Correlations between characteristics of CST lesion fractions and electrophysiological scores were calculated using the Spearman correlation coefficient in two different ways. First, we computed the correlations between lesion fractions in the CST (brain, cord and brain + cord) and the quantities from the matching side. Second, to assess the specificity of the lateralization, we also computed correlations between overall nonlateralized variables (whole brain, whole cord, whole central nervous system (CNS) when appropriate) and mean electrophysiological scores. The associated p values for $r = 0$ are also given.

Correlations between MRI metrics, electrophysiology and clinical scores were assessed using the Spearman correlation coefficient. The associated p values for $r = 0$ are also given.

Results

Clinical characteristics

We included 44 patients with RRMS. Their clinical characteristics are summarized in Table 1. Two of these patients had a motor deficit, and 17 had an isolated pyramidal syndrome with no motor deficit.

MRI characteristics

Lesion volume fractions

One patient was excluded from this analysis because motion artifacts on the spinal cord T2*w images prevented precise delineation of the lesions. The mean lesion number was 2.5 in the SC (range: 0-8; 6 patients had no spinal cord lesion) and 30 in the brain (range: 2-71). The mean lesion fraction was 5.64% (*SD* = 10.61) in the whole cervical SC and 0.26% (*SD* = 0.21) in the whole brain. Regarding the CST, mean absolute T2 lesion volumes were 52.5 mm^3 in the SC and 121.9 mm^3 in the brain. After normalizing for region volume, mean lesion fraction was 5.18% (*SD* = 10.05) in the SC CST and 0.88% (*SD* = 1.45) in the brain CST. Two patients had no CST lesions. Detailed results are provided in Table 2. Lesion volume fractions in the whole SC and the SC CST were strongly correlated (r = 0.96, 95% CI [0.93, 0.98], p < e-16). We also observed a similar, albeit less pronounced, correlation in the brain (r = 0.49, 95% CI [0.22, 0.69], p = 0.001). By contrast, we did not find any evidence of a correlation between the lesion volume fractions in the brain and SC (r = 0.06, 95% CI [-0.24, 0.36], p = 0.68).

DTI metrics in patients and controls

Table 3 gives the results of FA, RD and AD metrics for the SC and brain for patients and controls. In the whole cervical cord, we found evidence of differences between controls and patients for FA and RD, even after excluding lesions. When we focused on the CST, evidence of significant differences between the two groups vanished. In the whole brain and brain CST, we found no evidence of differences between controls' and patients' diffusion parameters. Moreover, we do not observe evidences of correlations between lesion fraction in the spinal cord and values of DTI metric in the spinal cord (Supplementary Table 2).

Electrophysiological scores

We collected electrophysiological data from 44 sides (21 right side and 23 left side). Four patients declined the electrophysiological assessment on one side, and one patient was excluded from the TST analysis because of repolarization abnormalities. The electrophysiological assessments are detailed in Supplementary Table 3. Twelve of the 24 patients (19 of the 44 sides) had at least one abnormal value (7/44 CMCT, 9/42 MEP ratio, and 15/42 TST ratio). Sides associated with pyramidal signs experienced lower mean TST ratio scores than sides without pyramidal signs (74.44, SD = 24.40 versus 95.34, SD = 11.13, p=4e-04, Table 4).

Associations between MRI metrics and clinical scores

Lesion volume fractions and clinical scores

Detailed correlations are provided in Table 5. EDSS was correlated with the lesion fraction of the whole SC (r = 0.41, p = 0.007). Pyramidal EDSS was positively correlated with the lesion fractions of the SC CST (r = 0.39, p = 0.01), whole SC (r = 0.34, p = 0.02) and brain + spine CST (r = 0.41, p = 0.007).

DTI parameters and clinical scores

We did not observe significant correlations between diffusion parameters and clinical data. (Supplementary Table 4).

Lateralized associations between MRI metrics and electrophysiology

Detailed correlations are provided in Table 6. CMCT was correlated with lesion fraction in the spine CST (r=0.33, p=0.03) and CNS (r = 0.49, p = 0.04). TST amplitude ratio and TST area were correlated with the lesion fraction in the brain CST (r = -0.34, p=0.03 and r = -0.40, p = 0.01). Both these electrophysiological parameters were also associated with the lesion fraction in the brain + spine CST (r = -0.39, p = 0.01 and r = -0.48, p = 0.002). Detailed correlations between clinical metrics and electrophysiology are provided in Supplementary Table 5.

Discussion

The main contribution of our study was to perform a description of CST damage from the primary motor cortex to the low cervical cord, quantifying both focal lesion load and diffuse tissue damage, as well as in the brain and SC. Moreover, we precisely assessed the impact of CST structural damage on patients' motor functions, by combining clinical tests and electrophysiology. The main conclusions of this work are threefold:

First, CST focal lesions were frequent, concerning 42 of the 44 patients with early RRMS. This result is in line with the literature[5,23], although previous studies only quantified brain CST lesion load. More importantly, we found that the lesion load was not homogeneously distributed along the CST. The T2 absolute lesion volume was about twice as high in the brain portion of the CST as in its SC portion. However, the volume of the cervical cord CST was also much lower than the volume of the brain CST. Thus, after normalization for each ROI volume, the focal damage proved to be far more pronounced in the SC portion of the CST than in the brain portion, indicating that the SC portion of the CST is vulnerable to lesions. Moreover, the lesion fractions in the SC CSTs were more closely correlated with pyramidal EDSS scores and CMCT than those in the brain CST, or even the brain + spine CST, emphasizing the highly functional aspect of the SC. We also found a close correlation between the SC CST lesion fraction and the whole cord lesion fraction. Owing to the small size of the spinal cord, a focal lesion is highly likely to impact the CST. Consequently, there was very little added value in specifically studying the CST lesion fraction compared with the whole SC lesion fraction in our study.

Second, we found evidence of differences in SC diffusion parameters between patients and controls, illustrating the presence of measurable focal as well as diffuse damage in the SC at the beginning of the disease. These results confirm a recent study where similar conclusions were reached using magnetization transfer ratio imaging[24]. By contrast, we did not observe any significant differences in brain WM diffusion parameters between patients and controls. Like the lack of correlation between the SC and brain lesion fractions, this result illustrates the value of not limiting damage analysis to the brain portion of the CNS to characterize patients' pathophysiological state. Previous studies[5,6,27] have reported evidence of patient-to-control differences on various diffusion parameters in brain WM, but these involved patients with more advanced disease (mean EDSS = 4, 2.8 and 1.5, compared with 0.8 in our population). When we specifically focused on the SC portion of the CST, we did not observe any significant differences in diffusion parameters between patients and controls. This result can probably partly be explained by the

low resolution of our DTI spinal cord imaging (2*2*2 mm^3) resulting in a notable partial volume effect and more variable DTI measurements.

Third, despite the high occurrence of CST structural damage in our cohort, only 50% of patients had electrophysiologically measurable functional consequences, 38% had a pyramidal syndrome, and 5% had a motor deficit. This can probably be explained by the varying degrees of demyelination and axonal loss in focal MS lesions reported in anatomopathological studies[25], leading to differing consequences in terms of conduction time or conduction block. In the present study, we used both CMCT[14], which reflects demyelination or loss of rapidly conducting corticospinal fibres, and the TST amplitude ratio, which reflects a conduction failure resulting from either central conduction block or axonal loss[15,16]. Accordingly, the TST ratio abnormalities were associated with pyramidal signs, whereas no association was found with the CMCT. These results were in line with a previous study[13]. However, the correlations between lesion fractions in the CST and electrophysiological parameters are more difficult to interpret, as lesion fraction does not specifically reflect demyelination or axonal loss. It would be worthwhile carrying out a precise quantification of lesion severity using quantitative MRI techniques such as submillimetric axial MT imaging in future studies, in order to better explain the link between MRI and electrophysiological parameters.

Limitations

First, our analysis did not include the thoracic segment of the SC. To date, the acquisition and postprocessing of thoracic SC images has proved more challenging than for the cervical portion[7]. Second, CST delineation is only an approximation, even using state-of-the-art techniques such as tractography for the brain and an atlas for SC[26]. Third, our sample consisted of 43 patients with early RRMS, and 16 controls for the brain and 19 for the SC acquisitions. This moderate sample size was nonetheless sufficient to highlight the stronger involvement of SC lesions in CST damage and motor function abnormalities, compared with brain lesions. Fourth, we only included patients with early RRMS in our study. Consequently, only two patients had a motor deficit, thus preventing us from evaluating the link between CST lesion load and clear motor disability. While this was beyond the scope of the present study, it would be worthwhile including patients with different MS phenotypes and more advanced disease in future studies. Moreover, our population consisted of patients who met criteria for disease severity (> 9 brain lesions and/or myelitis). Thus, we cannot exclude the possibility that these inclusion criteria introduced a bias toward an over-representation of focal SC lesions in our cohort. It will be important to reproduce these results in other cohorts.

Conclusions and perspectives

Our study described both the structural and functional involvement of the CST in the brain and cervical SC. Our results highlight the high frequency of focal CST damage even in the first few years of RRMS, as well as the major contribution of SC lesions to CST damage and motor function abnormalities. The link between early CST lesion volume fraction and subsequent motor disability will be evaluated in an ongoing longitudinal study.

References

1. Lublin FD, Reingold SC, Cohen JA, et al. Defining the clinical course of multiple sclerosis: the 2013 revisions. Neurology 2014;83(3):278–286.

2. Wilson M, Tench C, Morgan P and Blumhardt L. Pyramidal tract mapping by diffusion tensor magnetic resonance imaging in multiple sclerosis: improving correlations with disability. J Neurol Neurosurg Psychiatry 2003;74:203-207.

3. Fritz N, Keller J, Calabresi P and Zackowski K. Quantitative measures of walking and strength provide insight into brain corticospinal tract pathology in multiple sclerosis. NeuroImage Clin 2017;14:490-498.

4. Tovar-Moll F, Evangelou L, Chiu A, et al. Diffuse and focal corticospinal tract disease and its impact on patient disability in Multiple sclerosis. J Neuroimaging 2015;25:200-206.

5. Daams M, Steenwijk M, Wattjes M, et al. Unraveling the neuro-imaging predictors for motor dysfunction in longstanding multiple sclerosis. Neurology 2015;85:1-8.

6. Lin F, Yu C, Jiang T, et al. Diffusion tensor tractography-based group mapping of the pyramidal tract in relapsing remitting Multiple Sclerosis patients. Am J Neuroradiol 2007;28: 278-85.

7. Martin AR, Aleksanderek I, Cohen-Adad J, et al. Translating state-of-the-art spinal cord MRI techniques to clinical use: a systematic review of clinical studies utilizing DTI, MT, MWF, MRS, and fMRI. NeuroImage Clin 2016;10:192-238.

8. Kearney H, Altmann DR, Samson RS, et al. Cervical cord lesion load is associated with disability independently from atrophy in MS. Neurology 2015;84(4):367-73.

9. Brownlee WJ, Altmann DR, Alves Da Mota P, et al. Association of asymptomatic spinal cord lesions and atrophy with disability 5 years after a clinically isolated syndrome. Mult Scler. 2017 Apr;23(5):665-674.

10. Arrambide G, Rovira A, Sastre-Garriga J, et al. Spinal cord lesions: a modest contributor to diagnosis in clinically isolated syndromes but a relevant prognostic factor. Mult Scler 2017;23(5):665-674.

11. Zackowski K, Smith S, Calabresi P, et al Sensorimotor dysfunction in multiple sclerosis and column-specific magnetization transfer-imaging abnormalities in the spinal cord. Brain 2009;132(Pt 5):1200-9.

12. Naismith RT, Xu J, Klawiter EC, et al. Spinal cord tract diffusion tensor imaging reveals disability substrate in demyelinating disease. Neurology 2013;80(24):2201-9.

13. Rico A, Audoin B, Franques J, et al. Motor evoked potentials in clinically isolated syndrome suggestive of

multiple sclerosis. Mult.Scler 2009;15:355–362.

14. Kidd D, Thompson PD, Day BL, et al. Central motor conduction time in progressive multiple sclerosis. Correlations with MRI and disease activity. Brain 1998;121: 1109–1116.

15. Magistris MR, Rosler KM, Truffert A, et al. A clinical study of motor evoked potentials using a triple stimulation technique. Brain 1999;122: 265–279.

16. Buhler R, Magistris MR, Truffert A, et al. The triple stimulation technique to study central motor conduction to the lower limbs. Clin Neurophysiol 2001;112:938–949.

17. Polman C, Reingold SC, Banwell B, et al. Diagnostic criteria for multiple sclerosis: 2010 revisions to the McDonald criteria. Ann Neurol 2011; 69:292-302.

18. De Leener B, Lévy S, Dupont SM, et al. SCT: Spinal Cord Toolbox, an open-source software for processing spinal cord MRI data. Neuroimage 2017;145:27-43.

19. Commowick O, Wiest-Daessle N and Prima S. Block-matching strategies for rigid registration of multimodal medical images [Internet]. In: 2012 9th IEEE International Symposium on Biomedical Imaging (ISBI). 2012. Available from: http://dx.doi.org/10.1109/isbi.2012.6235644

20. Rossini P, Burke D, Chen R, et al. Non-invasive electrical and magnetic stimulation of the brain, spinal cord, roots and peripheral nerves: Basic principles and procedures for routine clinical and research application: An updated report from an I.F.C.N. Committee. Clinical Neurophysiology 2015;126(6):1071–1107.

21. Magistris MR, Rösler KM. Chapter 3 The triple stimulation technique to study corticospinal conduction. Supplements to Clinical Neurophysiology 2003 (Vol. 56).

22. https://www.r-project.org

23. Pagani E, Filippi M, Rocca MA and Horsfield MA. A method for obtaining tract-specific diffusion tensor MRI measurements in the presence of disease: application to patients with clinically isolated syndromes suggestive of multiple sclerosis. Neuroimage 2005;26(1):258-65.

24. Combès B, Kerbrat A, Ferré JC, et al. Focal and diffuse cervical spinal cord damage in patients with early relapsing–remitting MS: a multicentre magnetisation transfer ratio study. Mult Scler 2018 Jun 1:1352458518781999. doi: 10.1177/1352458518781999.

25. Frischer J, Weigand S, Guo Y, et al. Clinical and pathological insights into the dynamic nature of the white matter multiple sclerosis plaque. Ann Neurol 2015;78(5):710-721.

26. Lévy S, Benhamou M, Naaman C, et al. White matter atlas of the human spinal cord with estimation of partial volume effect. Neuroimage 2015;119:262-271.

27. Bommarito G, Bellini A, Pardini M, et al. Composite MRI measures and short-term disability in patients with clinically isolated syndrome suggestive of MS. Mult Scler 2017; 5:623–631.

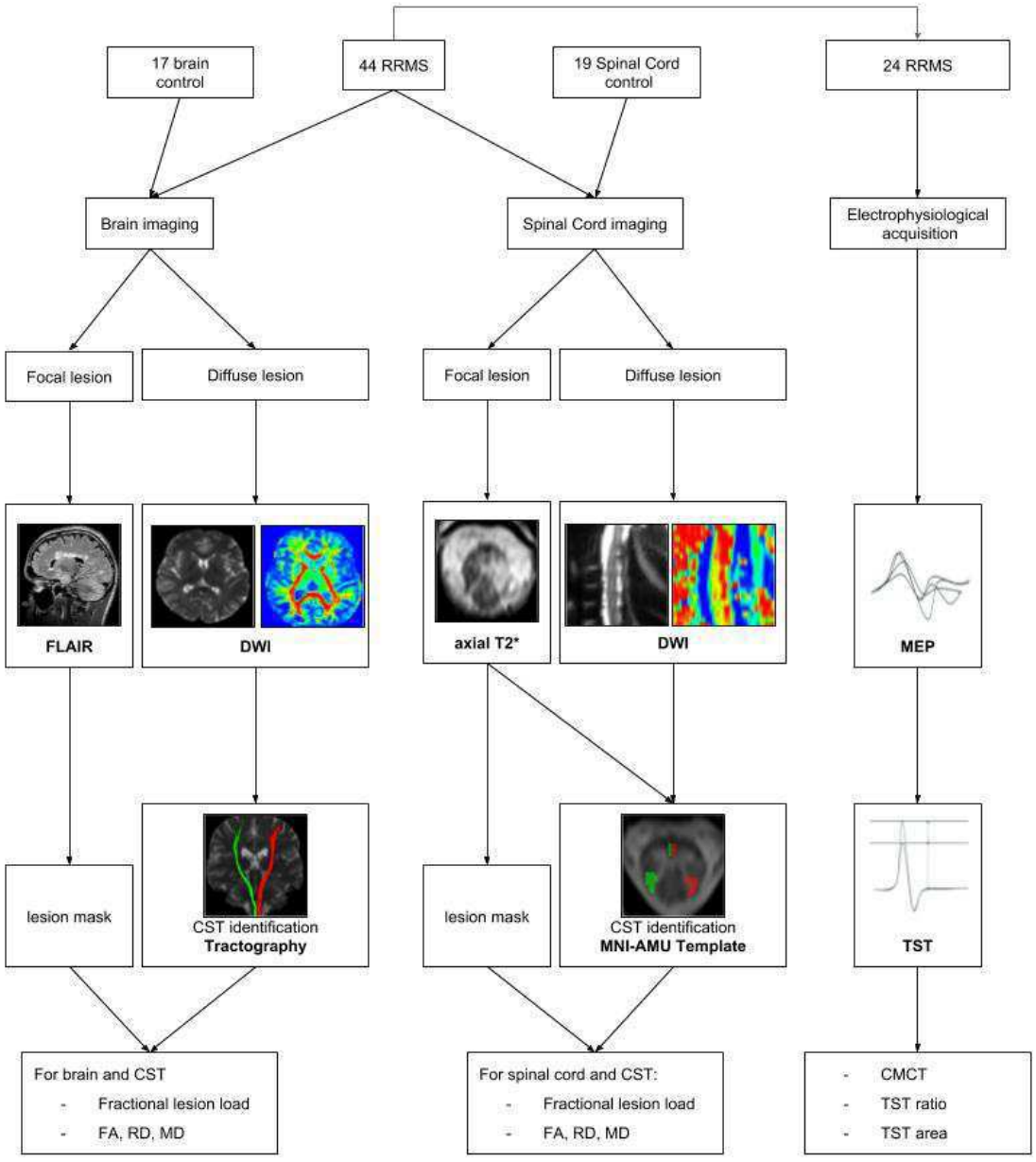

Figure 1: Study design.

RRMS = relapsing-remitting multiple sclerosis; DWI = diffusion-weighted imaging; CST = corticospinal tract; MEP = motor evoked potential; TST = triple stimulation technique; CMCT = central motor conduction time; FA = fractional anisotropy; RD = radial diffusivity; AD = axial diffusivity.

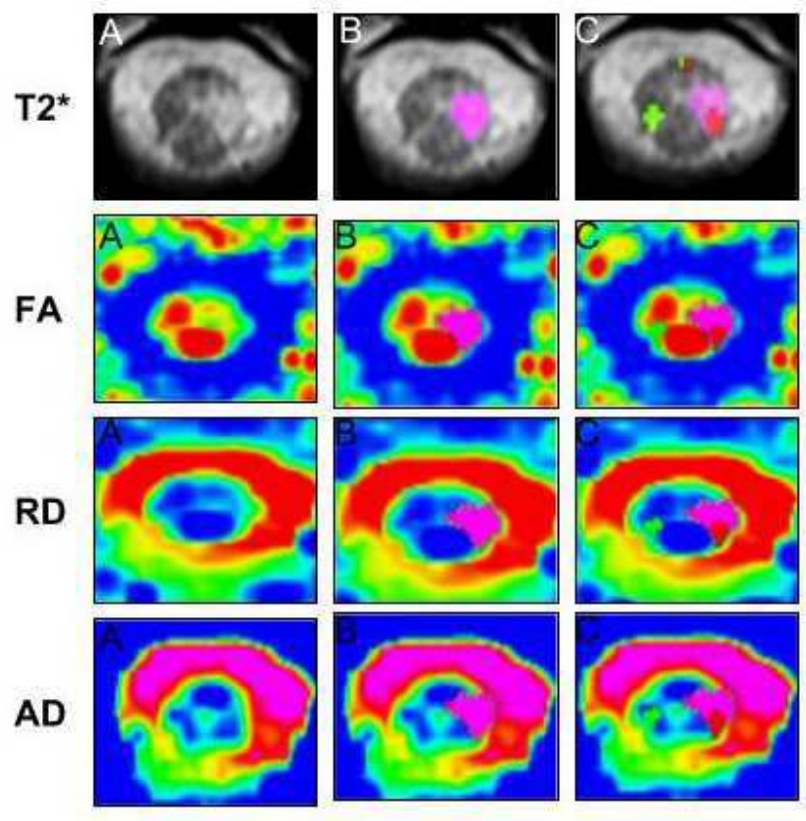

Figure 2: Example of spinal cord MRI in a patient with RMMS.

First row: axial T2*. Other rows: DTI parameter maps. A: native image; B: segmented lesion in pink; C: masks of corticospinal tract crossing the lesion (left CST in red, right CST in green). FA = fractional anisotropy; RD = radial diffusivity; AD = axial diffusivity.

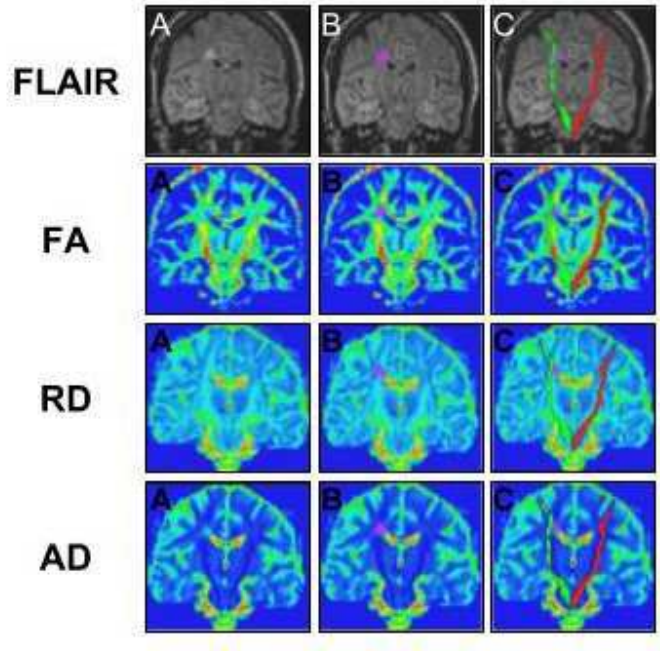

Figure 3: Example of brain MRI in patient with RRMS.

First row: FLAIR acquisition registered on b0 image. Other rows: parametric maps. A = native images; B = segmented lesion in pink; C = masks of corticospinal tract crossing the lesion (left CST in red, right CST in green); FA = fractional anisotropy; RD = radial diffusivity; AD = axial diffusivity.

Clinical characteristics (*N* = 44)		
Age (years)	Mean ± *SD*	30.7 ± 6.4
Sex	(F/M)	28/16
Disease duration (months)	Mean ± *SD*	21.1 ± 11.40
EDSS	median (range)	1 (0-3)
Pyramidal EDSS	median (range)	0 (0-2)
9-HPT right (s)	mean ± *SD* (range)	19.1± 4.4 (13.9-40.6)
9-HPT left (s)	mean ± *SD* (range)	19.7 ± 5.7 (14.5-54.1)
6MWT (m)	mean ± *SD* (range)	540 ± 95 (324-822)
T25FW (min)	mean ± *SD* (range)	4.9 ± 0.8 (3.8-7.8)
MSW12	mean ± *SD* (range)	17.2 ± 10.7 (12-54)
Right pyramidal signs	(yes/no)	8/36
Left pyramidal signs	(yes/no)	9/35
Disease modifying drugs	Fingolimod n=9; Interferon n=10; Glatiramer acetate n=11; Teriflunomid n= 6; Dimethyl fumarate n=3, Other n=4 (Rituximab, Natalizumab, Mycophenolic acid, Alemtezumab), no DMD n=1.	

Table 1: Clinical characteristics of patients.

EDSS = Expanded Disability Status Scale; T25FW = Timed 25-Foot Walk Test; 9HPT = 9-Hole Peg Test; 6MWT = 6-Minute Walking Test; MSW12 = MS Walking Scale.

		WHOLE		CST	
		Lesion volume in ROI (mm^3)	Percentage of lesions in ROI	Lesion volume in ROI (mm^3)	Percentage of lesions in ROI
Spinal cord	Mean ± *SD* (min, max)	425.20 ± 790.48 (0.00, 4160.23)	5.64 ± 10.61 (0.00, 57.00)	52.54 ± 99.67 (0.00, 568.16)	5.18 ± 10.45 (0.00, 62.44)
Brain	Mean ± *SD* (min, max)	3668.84 ± 3,292.29 (187.45, 16 916.51)	0.26 ± 0.21 (0.01, 1.00)	121.86 ± 214.08 (0.00, 976.00)	0.88 ± 1.45 (0.00, 5.44)
Spinal cord + Brain	Mean ± *SD* (min, max)	4094.04 ± 3435.63 (187.45, 17 080.47)	0.28 ±0.23 (0.01, 1.00)	174.40 ± 241.30 (0.00, 1207.26)	1.23 ± 1.71 (0.00, 7.60)

Table 2: Brain, spinal cord and corticospinal tract lesion volume.

White column: Mean, standard deviation and range for lesion volume in each ROI (in mm3). **Gray column:** Mean, standard deviation and range for lesion volume fraction in each ROI (i.e., percentage of lesions in ROI).

	Controls (Spinal cord: *n* = 18, Brain *n* = 16)	**Patients (*n* = 43)**	***p* value for no control-to-patient difference**
Spinal cord			
FA			
whole spinal cord	0.719 (0.054)	0.664 (0.079)	0.009
NASC	-	0.661 (0.081)	0.002
CST	0.746 (0.078)	0.712 (0.093)	0.180
lesion	-	0.655 (0.115)	-
RD (x 1000)			
whole spinal cord	0.406 (0.076)	0.483 (0.119)	0.014
NASC	-	0.492 (0.127)	0.002
CST	0.366 (0.114)	0.408 (0.138)	0.258
lesion	-	0.473 (0.149)	-
AD (x 100)			
whole spinal cord	0.158 (0.014)	0.158 (0.014)	0.946
NASC	-	0.159 (0.014)	0.760
CST	0.159 (0.014)	0.158 (0.016)	0.800
lesion	-	0.156 (0.018)	-

Brain			
FA			
WM	0.346 (0.025)	0.341 (0.020)	0.451
NAWM	0.346 (0.025)	0.342 (0.020)	0.518
CST	0.480 (0.025)	0.469 (0.024)	0.139
lesion	-	0.311 (0.038)	-
RD (x 1000)			
WM	0.610 (0.045)	0.613 (0.046)	0.791
NAWM	0.610 (0.045)	0.611 (0.046)	0.914
CST	0.548 (0.048)	0.556 (0.039)	0.533
lesion	-	0.870 (0.103)	-
AD (x 100)			
WM	0.105 (0.003)	0.105 (0.004)	0.623
NAWM	0.105 (0.003)	0.104 (0.004)	0.427
CST	0.120 (0.005)	0.120 (0.005)	0.679
lesion	-	0.139 (0.014)	-

Table 3: Mean (standard deviation) diffusion parameter values for patients and controls and *p* values associated with no differences between patients and controls.

FA = fractional anisotropy; RD = radial diffusivity; AD = axial diffusivity; NA = normal-appearing.

	Sides without pyramidal signs (n=31)	Sides with pyramidal signs (n=11)	p-value for no difference between the two groups
CMCT	6.29 (1.44)	7.54 (3.32)	0.09
TST ratio	98.30 (9.32)	75.46 (20.62)	1.3e-05
TST area	95.34 (11.13)	74.44 (24.40)	4.4e-04

Table 4: Mean (standard deviation) electrophysiological scores for sides without pyramidal signs and with pyramidal signs, as well as the *p* values associated with no differences between the two groups.

CMCT = central motor conduction time; TST = triple stimulation technique.

		EDSS	pyEDSS	MSWS12	9HPT	6MWT	25FTW
Spinal cord	**CST**	*r*=0.25 *p*=0.11	***r*=0.39** ***p*=0.01**	*r*=0.10 *p*=0.52	*r*=0.26 *p*=0.09	*r*=-0.22 *p*=0.15	*r*=0.11 *p*=0.50
	Whole spinal cord	***r*=0.41** ***p*=0.007**	***r*=0.34** ***p*=0.02**	*r*=0.26 *p*=0.09	*r*=0.20 *p*=0.20	*r*=-0.16 *p*=0.32	*r*=0.16 *p*=0.32
Brain	**CST**	*r*=0.08 *p*=0.62	*r*=0.16 *p*=0.30	*r*=0.01 *p*=0.95	*r*=0.18 *p*=0.26	*r*=-0.05 *p*=0.72	*r*=-0.06 *p*=0.72
	Whole brain	*r*=0.004 *p*=0.98	*r*=0.09 *p*=0.54	*r*=0.08 *p*=0.59	*r*=0.08 *p*=0.57	*r*=0.07 *p*=0.64	*r*=-0.03 *p*=0.87
Spinal cord + Brain	**CST**	*r*=0.24 *p*=0.12	***r*=0.41** ***p*=0.007**	*r*=0.16 *p*=0.32	*r*=020 *p*=0.20	*r*=-0.04 *p*=0.79	*r*=0.04 *p*=0.79
	Whole	*r*=0.10 *p*=0.50	*r*=0.23 *p*=0.14	*r*=0.12 *p*=0.46	*r*=0.12 *p*=0.43	*r*=-0.01 *p*=0.93	*r*=-0.01 *p*=0.93

Table 5: Correlation coefficients and *p* values between lesion volume fractions and clinical scores

Significant results are indicated in bold. EDSS = Expanded Disability Status Scale; T25FW = Timed 25-Foot Walk Test; 9HPT = 9-Hole Peg Test; 6MWT = 6-Minute Walking Test; MSW12 = MS Walking Scale; AMSQ = Arm Function in MS Questionnaire.

	LESION FRACTION					
	SPINAL CORD		BRAIN		BRAIN + SPINAL CORD	
	ALL	Lateralized CST	ALL	Lateralized CST	ALL	Lateralized CST
CMCT	*r*=0.35 *p*=0.15	***r*=0.33** ***p*=0.03**	*r*=0.29 *p*=0.23	*r*=-0.02 *p*=0.89	***r*=0.49** ***p*=0.04**	*r*=0.21 *p*=0.20
TST ratio	*r*=-0.15 *p*=0.54	*r*=-0.23 *p*=0.15	*r*=-0.07 *p*=0.79	***r*=-0.34** ***p*=0.03**	*r*=-0.07 *p*=0.80	***r*=-0.39** ***p*=0.01**
TST area	*r*=-0.17 *p*=0.50	*r*=-0.25 *p*=0.12	*r*=-0.11 *p*=0.66	***r*=-0.40** ***p*=0.01**	*r*=-0.12 *p*=0.63	***r*=-0.48** ***p*=0.002**

Table 6: Correlations between electrophysiological data and lesion fractions in spinal cord, brain and central nervous system.

Significant values are indicated in bold. Lateralized CST = corresponding functional corticospinal tract. CMCT = central motor conduction time; TST = triple stimulation technique.

		Patients		Spinal cord MRI controls	Brain MRI controls
		MRI	Electrophysiology		
Number		44	24/44	19	16
Sex F/M		28/16	13/11	11/8	11/5
Age (years)	Mean ± *SD*	30.7 ± 6.4	33.3 ± 5.9	33.7 ± 7.8	39.3 ± 9.1

Supplementary Table 1: Summary of participants' demographic characteristics.

SPINE		All spine lesion fraction
Mean FA	lesion	*r=0.068* *p=0.694*
	all spine	*r=*-0.048 *p=0.759*
Mean RD	lesion	*r=-0.029* *p=0.865*
	all spine	*r=0.08* *p=0.961*
Mean AD	lesion	*r=-0.016* *p=0.924*
	all spine	*r=-0.120* *p=0.445*

Supplementary Table 2: Correlations between DTI metrics of the spinal cord and lesion fraction of the spinal cord
FA = fractional anisotropy; RD = radial diffusivity; AD = axial diffusivity.

		Right	Left	Total
CMCT (ms)	Mean ± *SD*	*n* = 20 6.6 ± 2.4	*n* = 22 6.7 ± 1.9	*n* = 42 6.6 ± 2.1
	(range)	(3.3-14.4)	(3.7-12.9)	(3.3-14.4)
TST ratio (%)	Mean ± *SD*	*n* = 20 91.1 ± 15.1	*n* = 22 93.4 ± 17.9	*n* = 42 92.3 ± 16.5
	(range)	(45.3-110.3)	(33.3-121.3)	(33.3-121.3)
TST area (%)	Mean ± *SD*	*n* = 20 89.2 ± 18.3	*n* = 22 90.5 ± 18.1	*n* = 42 89.9 ± 17.9
	(range)	(39.9-110.3)	(28.8-117.2)	(28.8-117.2)

Supplementary Table 3: Electrophysiological scores.

CMCT = central motor conduction time; TST = triple stimulation technique.

		EDSS	PyEDSS	MSWS12	9HPT	6MWT	25FTW	AMSQ
FA	Whole Cord	*r*=-0.155 *p*=0.321	*r*=0.067 *p*=0.669	*r*=-0.206 *p*=0.185	*r*=0.273 *p*=0.077	*r*=0.124 *p*=0.428	*r*=-0.043 *p*=0.782	*r*=-0.146 *p*=0.516
	Cord CST	*r*=-0.073 *p*=0.641	*r*=-0.007 *p*=0.964	*r*=-0.212 *p*=0.171	*r*=0.157 *p*=0.314	*r*=0.022 *p*=0.889	*r*=0.012 *p*=0.937	*r*=0.042 *p*=0.854
	Brain All	*r*=-0.004 *p*=0.980	*r*=0.013 *p*=0.933	*r*=-0.047 *p*=0.764	*r*=-0.367 *p*=0.016	*r*=-0.116 *p*=0.460	*r*=0.097 *p*=0.535	*r*=-0.230 *p*=0.303
	Brain CST	*r*=-0.077 *p*=0.622	*r*=-0.060 *p*=0.703	*r*=-0.277 *p*=0.073	*r*=-0.070 *p*=0.654	*r*=-0.076 *p*=0.626	*r*=0.004 *p*=0.982	*r*=0.115 *p*=0.611
RD	Whole cord	*r*=0.036 *p*=0.819	*r*=-0.137 *p*=0.380	*r*=0.100 *p*=0.524	*r*=-0.288 *p*=0.061	*r*=-0.034 *p*=0.830	*r*=-0.037 *p*=0.816	*r*=0.058 *p*=0.796
	Cord CST	*r*=-0.026 *p*=0.871	*r*=-0.033 *p*=0.835	*r*=0.168 *p*=0.282	*r*=-0.151 *p*=0.332	*r*=-0.002 *p*=0.989	*r*=-0.040 *p*=0.798	*r*=-0.160 *p*=0.477
	Brain All	*r*=-0.068 *p*=0.666	*r*=-0.027 *p*=0.896	*r*=-0.158 *p*=0.313	*r*=0.226 *p*=0.145	*r*=0.290 *p*=0.059	*r*=-0.184 *p*=0.238	*r*=0.230 *p*=0.303
	Cord CST	*r*=0.012 *p*=0.940	*r*=0.037 *p*=0.812	*r*=0.155 *p*=0.320	*r*=-0.004 *p*=0.979	*r*=0.081 *p*=0.604	*r*=0.005 *p*=0.976	*r*=0.130 *p*=0.564
AD	Cord All	*r*=-0.056 *p*=0.722	*r*=0.002 *p*=0.990	*r*=0.004 *p*=0.978	*r*=-0.083 *p*=0.596	*r*=0.026 *p*=0.867	*r*=-0.062 *p*=0.691	*r*=-0.059 *p*=0.793
	Cord CST	*r*=-0.054 *p*=0.729	*r*=-0.007 *p*=0.965	*r*=0.074 *p*=0.639	*r*=0.003 *p*=0.982	*r*=0.046 *p*=0.768	*r*=-0.053 *p*=0.734	*r*=-0.065 *p*=0.772
	Brain All	*r*=-0.099 *p*=0.528	*r*=-0.030 *p*=0.851	*r*=-0.238 *p*=0.124	*r*=0.214 *p*=0.168	*r*=0.334 *p*=0.028	*r*=-0.206 *p*=0.184	*r*=0.195 *p*=0.383
	Brain Cst	*r*=-0.298 *p*=0.052	*r*=-0.226 *p*=0.144	*r*=-0.272 *p*=0.077	*r*=-0.179 *p*=0.251	*r*=0.162 *p*=0.300	*r*=-0.097 *p*=0.537	*r*=0.126 *p*=0.576

Supplementary Table 4: Correlation coefficients and *p* values between DTI parameters and clinical scores. CST = corticospinal tract; FA = fractional anisotropy; RD = radial diffusivity; AD = axial diffusivity; EDSS = Expanded Disability Status Scale; T25FW = Timed 25-Foot Walk Test; 9HPT = 9-Hole Peg Test; 6MWT = 6-Minute Walking Test; MSW12 = MS Walking Scale; AMSQ = Arm Function in MS Questionnaire.

	EDSS	pyEDSS	MSW12	9HPT	6MWT	25FTW
CMCT	0.303 *p*=0.051	**0.383** *p*=0.012	**0.414** *p*=0.006	0.193 *p*=0.221	-0.190 *p*=0.229	**0.383** *p*=0.012
TST ratio	**-0.320** *p*=0.039	**-0.468** *p*=0.002	-0.098 *p*=0.538	0.088 *p*=0.579	0.085 *p*=0.592	-0.026 *p*=0.872
TST area	-0.303 *p*=0.052	**-0.548** *p*<0.001	-0.143 *p*=0.365	0.293 *p*= 0.60	0.136 *p*=0.391	-0.069 *p*=0.665

Supplementary Table 5: Correlations between electrophysiological and clinical data.

Significant values are indicated in bold. pyEDSS = pyramidal EDSS; T25FW = Timed 25-Foot Walk Test; 9HPT = 9-Hole Peg Test; 6MWT = 6-Minute Walking Test; MSW12 = MS Walking Scale; AMSQ = Arm Function in MS Questionnaire.

Appendix for MRI methodology

for

Joint assessment of brain and spinal cord motor tract damage in patients with early RRMS:

predominant impact of spinal cord lesions on motor function

1/ Hardware
Siemens MAGNETOM Verio (VB17) 3T
Coil head and surface (number of coil channels: 12, 32)

2/ Acquisitions sequences
3D FLAIR
Acquisition time=5min
Orientation=Sagittal
Voxel size=1x1x1.1
TR=5000
TE=399
TI=1800
Flip angle=120
Field of view=256x256
Matrix size=256x256
3DT1
Acquisition time=4:30
Orientation=Sagittal
Voxel size=1x1x1
TR=1900
TE=2.26
TI=900
Flip angle=9
Field of view=256x256
Matrix size=256x256
Acquisitions both (pre and post Gd) Contrast enhancement
Axial T2
Acquisition time=2:12

Orientation=Axial
Voxel size=0.7x0.7x3
TR=6530
TE=9.4/84
Flip angle=148
Field of view=220x165
Matrix size=320x240
DTI- Single-shot GRE EPI
Acquisition time=5:47
Orientation=Sagittal
Voxel size=2x2x2
TR=11000
TE=82
b min /b max=0/1000
Number of directions =30
Flip angle=90
Field of view=256x256
Matrix size=128x128
Spinal cord acquisition sequence Axial T2*W MEDIC
2 acquisitions= C1-C3 and C4-C7
Acquisition time=twice 4min
Orientation=Axial
Voxel size=0.7x0.7x3
TR=849
TE=23
Flip angle=30
Field of view=180x180
Matrix size=256x256
Spinal cord acquisition sequence Sag T2
2 acquisitions = Cervical and Dorsal
Acquisition time=3min each
Orientation=Sagittal
Voxel size=0.9x0.7x2.5
TR=3000
TE=68
Flip angle=180

Field of view=260x260 Matrix size=384x75
Spinal cord acquisition sequence Sag PSIR
2 acquisitions: Cervical and Dorsal Acquisition time=2:37s each Orientation=Sagittal Voxel size=0.8x0.8x2.5 TR=4585ms TE=9.8ms TI=400ms Flip angle=160 Field of view=260x260 Matrix size=320x320
Spinal cord acquisition sequence DTI
Acquisition time= 6:29 Orientation=Sagittal Voxel size=2x2x2 TR=3600 TE=90 b min/b max=0/900 number of directions=30 Flip angle=23 Field of view=640x640 Matrix size=80x80
Spinal cord acquisition sequence 3D T1 MPRAGE
Acquisition time=4:12s Orientation=Sagittal Voxel size=1x1x1 TR=1800 TE=2.79 TI=900 Flip angle=9 Field of view=250x250 Matrix size=256x256

3/ Image analysis methods and outputs	
Brain Lesions	
Brain lesion T2-hyperintense lesions were defined as abnormal areas of increased signal change that could be demarcated from the surrounding tissue on 3D FLAIR images. axial T2 weighted images and axial PD weighted images were used to help lesion identification but the final delineation was manually performed by RC and AK on the axial T2* images.	
Analysis software	ITK-snap (http://www.itksnap.org/)
Output measure	Brain lesion location, count and volume (mm^3)
Spinal cord lesions	
Focal spinal cord T2-hyperintense lesions were defined as abnormal areas of increased signal change that could be demarcated from the surrounding tissue on axial T2* images. Sagittal T2 weighted images and sagittal PSIR images were used to help lesion identification but the final delineation was manually performed by RC and AK on the axial T2* images.	
Analysis software	ITK-snap (http://www.itksnap.org/)
Output measure	Cervical spinal cord lesion location, count and volume (mm^3)
Brain DTI motion and distortion correction	
Motion and distortion correction with animaDiffusionImagePreprocessing using images with reversed phase encoding directions (antero-posterior and posterior-anterior)	
Analysis software	Anima (https://github.com/Inria-Visages/Anima-Public)
Output	- DTI images corrected - Estimated tensors map
Brain cortical and white matter segmentation for Primary motor area segmentation	
Brain cortical parcellation on T1 3D brain images using FreeSurfer. Primary motor area considered was the pre and para central areas.	
Analysis software	FreeSurfer (https://surfer.nmr.mgh.harvard.edu/)
Output	- Seeds for probabilistic tractography - White matter masks
Brain CST identification	
Brain portions of the CSTs were identified using probabilistic tractography (animaDTIProbabilisticTractography) on DTI images after lesion removing and using motor cortex as seeds. Fibers were then filtered through manually edited masks (ITK-snap) of brain pedoncula (left and right), anterior pons, and medulla oblongata (left and right)	
Analysis software	- Anima (https://github.com/Inria-Visages/Anima-Public) - ITK-snap (http://www.itksnap.org/)
Output	- Brain CSTs location and volume for each patients and each sides
Brain and spinal cord DTI scalar maps	
Fractional anisotropy (FA), axial (AD) and radial diffusivity (RD) maps were obtained from a tensor image using *animaComputeDTIScalarMaps* and extracted on a set of prespecified ROIs.	
Analysis software	- Anima (https://github.com/Inria-Visages/Anima-Public)
Output	- mean FA, AD, RD for brain white matter, brain NASC, brain lesions and for spinal cord, normal appearing SC and SC lesions.

	- mean FA, AD, RD for brain and spinal cord CSTs.
Distortion and motion correction of spinal cord DTI images	
Motion and distortion correction of spinal cord DTI acquisition were performed using HySCO	
Analysis software	- HySCO (http://www.diffusiontools.com/documentation/hysco.html)
Output	- DTI images corrected - Estimated tensors map
Cord segmentation and vertebrae levels labeling on Spinal cord axial T2* and DTI b=0	
The whole cord (WC) was segmented using the automatic *sct_deepseg_sc* command. Then, the vertebrae were labeled using the *sct_label_vertebrae* command with initialization by selecting the axial slice that passed through the center of the C3C4 disc.	
Analysis software	- SCToolbox (https://sourceforge.net/p/spinalcordtoolbox/wiki/tools/)
Output	- Spinal cord mask and vertebrae labels
Identification of spinal cord CSTs Spinal cord axial T2* and DTI b=0 using atlas registration	
Spinal cord CSTs were identified using registration (SCT_register_to_template) from MNI-poly-AMU template to T2* and DTI b=0. Spinal cord CSTs were identified from c1 to c6.	
Analysis software	- SCToolbox (https://sourceforge.net/p/spinalcordtoolbox/wiki/tools/)
Output	Spinal cord CSTs - lateral and ventral CSTs for axial T2* - lateral CSTs for DTI
Alignment of spinal cord lesions on DTI images	
Lesions mask was registered to b=0 DTI images using sct_register_multimodal with the help of spinal cord segmentation already obtained from *sct_deepseg_sc*	
Analysis software	- SCToolbox (https://sourceforge.net/p/spinalcordtoolbox/wiki/tools/)
Output	- Spinal cord lesions mask on DTI images
Data extraction:lesion volume and mean DTI values	
Mean DTI values were extracted using FSL on DTI scalar maps (FA, AD,RD) maps. Lesions volume on brain, spinal cord and corresponding CSTs were extracted using FSL	
Analysis software	- FSL https://fsl.fmrib.ox.ac.uk/fsl/fslwiki
Output	- Mean DTI values - Lesions volume

4/ Statistical analysis:
Statistical analyses were performed with R 3.4.3. (https://cran.r-project.org/)

Appendix for electrophysiology methodology for

Joint assessment of brain and spinal cord motor tract damage in patients with early RRMS: predominant impact of spinal cord lesions on motor function

Electrophysiological parameters were recorded using a Nicolet EDX apparatus (Natus Medical, Madison, Wisconsin, USA) and the dedicated software for Triple stimulation technique. A Magstim 200 Mono Pulse stimulator (maximum output 2.0 T) with a circular coil (Magstim Company, Whitland, Wales, UK) was used for Transcranial Magnetic Stimulation (TMS). Recordings were performed on each side on the first dorsal interosseous muscle using surface electrodes. To account for a possible partial volume effect, the median nerve was stimulated simultaneously [1]. The peripheral stimuli were applied over the ulnar nerve at the wrist and over the brachial plexus (using monopolar stimulation) and the descending volleys were respectively denoted $CMAP_{Erb}$ and $CMPAP_{wrist}$.

Motor evoked potentials (MEP): The overall procedure for TMS followed recommendations of International Federation of Clinical Neurophysiology [2]. For TMS, the coil was first placed over the vertex then moved slightly in all directions until the position yielding the largest response was found. TMS pulses began at 30% of the maximum output then were increased by steps of 10% until TMS evoked consistently MEPs, usually 120% of resting motor threshold. Latencies were determined with the shortest stable motor responses. Peripheral responses and MEPs were first elicited at rest for delay calculation. For some patients, facilitation maneuvers were needed to elicit MEPs (e.g slight contraction). In order to apply the same facilitation maneuvers during the peripheral stimulation than during TMS, strength contraction was monitored with audible surface electromyography.

MEP ratio was calculated as the baseline-to-peak amplitude of the MEP expressed as a percentage of the $CMAP_{wrist}$. The central motor conduction time was calculated with the F-wave technique using the following formula : CMCT = cortical MEP latency – (F-wave latency + CMAP distal Latency – 1)/2

Triple stimulation technique : TST was performed according to the technique described by Magistris [3]. Briefly, the technique consists in three stimuli applied successively with precise time-intervals calculated using the following formulas:

Delay 1 (brain/distal nerve stimulations) = minimum MEP latency– $CMAP_{wrist}$

Delay 2 (proximal/distal nerve stimulations) = $CMAP_{erb} - CMAP_{wrist}$

The TST_{test} curve was obtained with a first stimulation using cortical TMS that elicited descending volleys collided against elicited ascending volleys evoked at the ulnar wrist after Delay 1. A third stimulation at Erb's point, after a second interval corresponding to Delay 2, collided with the remaining ascending volleys. For the control conditions

($TST_{control}$ curve), the first stimulus was a sub maximal electrical stimulus applied at Erb's point and the second electrical stimulus at wrist was applied with Delay 2. The TST_{test} curve was compared with the $TST_{control}$ curve. Results were expressed as a percentage of the control $CMAP_{Erb}$ value: $TST_{test}/TST_{control.}$ This variable was named the TST ratio (%) for the amplitude ratio and as TST area for the area ratio.

References:

1. Humm A M, Z'Graggen, W J, Von Hornstein, N E, Magistris M R, Rösler K M. Assessment of central motor conduction to intrinsic hand muscles using the triple stimulation technique: Normal values and repeatability. Clinical Neurophysiology 2004;115:2558–2566.

2. Rossini P M, Burke D, Chen R et al. Non-invasive electrical and magnetic stimulation of the brain, spinal cord, roots and peripheral nerves: Basic principles and procedures for routine clinical and research application: An updated report from an I.F.C.N. Committee. Clinical Neurophysiology, 2015;126(6):1071–1107.

3. Magistris M R, Rösler K M. Chapter 3 The triple stimulation technique to study corticospinal conduction. Supplements to Clinical Neurophysiology 2003;Vol. 56,Chapter 3.

Résumé

Contexte: Bien que l'on soupçonne un impact cumulatif, l'effet des lésions du faisceau cortico-spinal (FCS) a été évalué séparément dans le cerveau et la moelle épinière chez les patients atteints de SEP. **Objectif:** Evaluer les dommages causés par les lésions de SEP sur le FCS encéphalique et médullaire cervical et examiner les associations relatives avec la fonction motrice, mesurée à la fois cliniquement et par électrophysiologie. **Méthodes:** Nous avons inclus 43 patients atteints de SEP rémittente récurrente diagnostiqué récemment. Les lésions ont été segmentées manuellement sur les IRM médullaire (T2 axiale *) et cérébral (3D FLAIR). Le FCS était automatiquement segmenté à l'aide d'un atlas (moelle) ou par tractographie (cerveau). Les fractions volumiques des lésions et les paramètres de diffusion ont été calculés pour la moelle, le cerveau et les FCS. La durée de conduction motrice centrale (CMCT) et le rapport d'amplitude mesuré par triple stimulation ont été mesurés pour 42 membres supérieurs, sur 22 patients. **Résultats:** Les fractions volumiques moyennes des lésions étaient de 5,2% dans la partie médullaire du FCS et de 0,9% dans la partie cérébrale. Nous n'avons pas trouvé de corrélation significative entre la fraction volumique des lésions du cerveau et de la moelle (r = 0,06, p = 0,68). Le score EDSS pyramidal et le CMCT étaient tous deux corrélés de manière significative avec la fraction lésionnelle du FCS médullaire (r = 0,39, p = 0,01 et r = 0,33, p = 0,03) mais pas avec la fraction lésionnelle du FCS encéphalique**. Conclusion:** Nos résultats mettent en évidence la contribution majeure des lésions médullaires du FCS sur la fonction motrice.

Abstract

Background: In patients with MS, the effect of structural damage to the corticospinal tract (CST) has been separately evaluated in the brain and spinal cord (SC), even though a cumulative impact is suspected. **Objective:** To evaluate CST damages on both the cortex and cervical SC, and examine their relative associations with motor function, measured both clinically and by electrophysiology. **Methods:** We included 43 patients with early relapsing-remitting MS. Lesions were manually segmented on SC (axial T2*) and brain (3D FLAIR) scans. The CST was automatically segmented using an atlas (SC) or tractography (brain). Lesion volume fractions and diffusion parameters were calculated for SC, brain and CST. Central motor conduction time (CMCT) and triple stimulation technique amplitude ratio were measured for 42 upper limbs, from 22 patients. **Results:** Mean lesion volume fractions were 5.2% in the SC portion of the CST and 0.9% in the brain portion. We did not find a significant correlation between brain and SC lesion volume fraction ($r = 0.06$, $p = 0.68$). The pyramidal EDSS score and CMCT were both significantly correlated with the lesion fraction in the SC CST ($r = 0.39$, $p = 0.01$ and $r = 0.33$, $p = 0.03$), but not in the brain CST. **Conclusion:** Our results highlight the major contribution of SC lesions to CST damage and motor function abnormalities.

U.F.R. DE **MEDECINE** DE RENNES | N°

CHOUTEAU, Raphaël - Évaluation conjointe des lésions du tractus moteur du cerveau et de la moelle épinière chez les patients atteints de SEP débutante: impact prédominant des lésions de la moelle épinière sur la fonction motrice

Feuilles : 47, illustrations : 3, tableaux : 11, 30 cm.- Thèse : Médecine ; Rennes 1; 2019 ; N° .

Résumé français

Contexte: Bien que l'on soupçonne un impact cumulatif, l'effet des lésions du faisceau cortico-spinal (FCS) a été évalué séparément dans le cerveau et la moelle épinière chez les patients atteints de SEP.

Objectif: Evaluer les dommages causés par les lésions de SEP sur le FCS encéphalique et médullaire cervical et examiner les associations relatives avec la fonction motrice, mesurée à la fois cliniquement et par électrophysiologie.

Méthodes: Nous avons inclus 43 patients atteints de SEP rémittente récurrente diagnostiqué récemment. Les lésions ont été segmentées manuellement sur les IRM médullaire (T2 axiale *) et cérébral (3D FLAIR). Le FCS était automatiquement segmenté à l'aide d'un atlas (moelle) ou par tractographie (cerveau). Les fractions volumiques des lésions et les paramètres de diffusion ont été calculés pour la moelle, le cerveau et les FCS. La durée de conduction motrice centrale (CMCT) et le rapport d'amplitude mesuré par triple stimulation ont été mesurés pour 42 membres supérieurs, sur 22 patients.

Résultats: Les fractions volumiques moyennes des lésions étaient de 5,2% dans la partie médullaire du FCS et de 0,9% dans la partie cérébrale. Nous n'avons pas trouvé de corrélation significative entre la fraction volumique des lésions du cerveau et de la moelle ($r = 0,06$, $p = 0,68$). Le score EDSS pyramidal et le CMCT étaient tous deux corrélés de manière significative avec la fraction lésionnelle du FCS médullaire ($r = 0,39$, $p = 0,01$ et $r = 0,33$, $p = 0,03$) mais pas avec la fraction lésionnelle du FCS encéphalique. Conclusion: Nos résultats mettent en évidence la contribution majeure des lésions médullaires du FCS sur la fonction motrice.

.

Rubrique de classement : NEUROLOGIE

Mots-clés : Lésion T2, électrophysiologie, IRM, Moelle épinière

Mots-clés anglais MeSH : T2 lesions, electrophysiology, MRI, spinal cord, multiple sclerosis

JURY : Président : Monsieur Gilles EDAN

Assesseurs : Mme Anne KERBRAT [directeur de thèse]
M. Paul SAULEAU
M. Jean-Christophe FERRE
M. Benoit COMBES